Scientific Research Publishing

Open Journal of Civil Engineering, 2022, 12, 587-614
https://www.scirp.org/journal/ojce
ISSN Online: 2164-3172
ISSN Print: 2164-3164

The Effects of Nanoparticle Additives on Thermophysical Properties of Concrete Mixtures

Kamran Rahmati Shadbad[1], Ali Foroughi-Asl[1], Siamak Talatahari[1], Sassan Mohasseb[2]

[1]Faculty of Civil Engineering, University of Tabriz, Tabriz, Iran
[2]ETH, SMTEAM GmbH, Meilen, Switzerland
Email: rahmati_kr@yahoo.com, aforough@tabrizu.ac.ir, siamak.talatahari@tabrizu.ac.ir, smteam.gmbh@gmail.com

How to cite this paper: Shadbad, K.R., Foroughi-Asl, A., Talatahari, S. and Mohasseb, S. (2022) The Effects of Nanoparticle Additives on Thermophysical Properties of Concrete Mixtures. *Open Journal of Civil Engineering*, **12**, 587-614.
https://doi.org/10.4236/ojce.2022.124033

Received: November 29, 2022
Accepted: December 27, 2022
Published: December 30, 2022

Abstract

In recent years, energy-retrofitting is becoming an imperative aim for existing buildings worldwide and increased interest has focused on the development of nanoparticle blended concretes with adequate mechanical properties and durability performance, through the optimization of concrete permeability and the incorporation of the proper nanoparticle type in the concrete matrix. In order to investigate the potential use of nanocomposites as dense barriers against the permeation of liquids into the concrete, three types of nanoparticles including Zinc Oxide (ZnO), Magnesium Oxide (MgO), and composite nanoparticles were used in the present study as partial replacement of cement. Besides, the effect of adding these nanoparticles on both pore structure and mechanical strengths of the concrete at different ages was determined, and scanning electron microscopy (SEM) images were then used to illustrate the uniformity dispersion of nanoparticles in cement paste. It was demonstrated that the addition of a small number of nanoparticles effectively enhances the mechanical properties of concrete and consequently reduces the extent of the water permeation front. Finally, the behavioral models using Genetic Algorithm (GA) programming were developed to describe the time-dependent behavioral characteristics of nanoparticle blended concrete samples in various compressive and tensile stress states at different ages.

Keywords

Nanoparticle Blended Concretes, Zinc Oxide (ZnO), Magnesium Oxide (MgO), Composite Nanoparticles, Genetic Algorithm (GA) Programming, Time-Dependent Behavioral Model

1. Introduction

Nanosized particles are often incorporated into cement paste, mortar, or other conventional construction materials with different characteristics; such material can possess advanced or smart properties required for the construction of high rise, long spans or intelligent/multifunctional structures, as well as make them more environmentally friendly systems (**Figure 1**). The introduction of nano-particles in cement paste and concrete mixtures might lead to some ways of enhancing the mechanical properties and durability of modern concrete [1] [2]. However, less attention has been paid to the application of nanotechnology in a cement matrix and concrete for the purpose of energy retrofitting and greater sustainability. Nanoparticles have a high surface area to volume ratio as well as higher surface energy compared with cement particles, providing the potential for tremendous chemical reactivity.

Due to the high thermal insulation characteristics of nanoparticles, these materials can be utilized effectively to reduce heating losses in buildings and structures, which requires high thermal resistance. Although a great deal of research has been carried out on the beneficial effects of the incorporation of silicon dioxide (SiO_2) and titanium oxide (nano-TiO_2) nanoparticles in cement-based composites, there are a few works about the influence of the other nanostructured metal oxides in concrete mixtures [3]-[8]. Therefore, these thermophysical effects of adding nanomaterial additives need to be carefully assessed with respect to all types of nanoparticles.

The incorporation of zinc-oxide nanoparticles as a replacement for cement has been investigated by Flores-Velez and Dominguez [9]. The mechanical strengths and pressure-sensitive properties of cement mortars with nano-SiO_2 (NS) and nano-Fe_2O_3 (NF) nanoparticles were experimentally studied by Li *et al.* [10]. Their results indicated that the average 28-day compressive and flexural strengths of cement mortar mixed with nano-SiO_2 and nano-Fe_2O_3 were both higher than that of plain cement mortar with the same water ratio. Furthermore, the abrasion resistance of plain concrete containing Titanium oxide (TiO_2) and Silicon dioxide (SiO_2) nanoparticles was also assessed by Li *et al.* [11]. It was

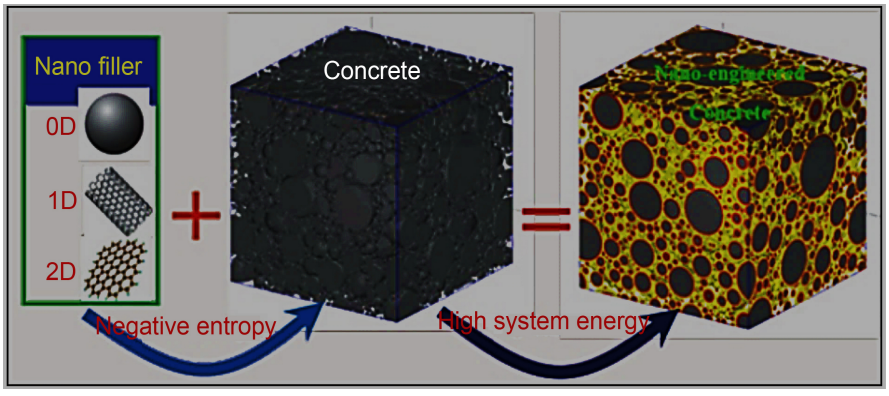

Figure 1. The schematic view of nano-engineered concrete [4].

demonstrated that the enhanced extent of the abrasion resistance of concrete decreases with the increasing content of nano-particles. The concrete containing nano-TiO_2 revealed a higher abrasion resistance in comparison with that containing the same amount of nano-SiO_2.

Owing to the high sensitivity of thermal conductivity to the effective water content of concrete, the nanomaterials are strongly recommended for the use in insulation systems. Previous studies have reported that by increasing the NS content, the air content increased and the apparent density subsequently decreased, while the size of NS particles has minimal effect on the air content and apparent density. Moreover, the dependence of the thermal conductivity on moisture content has been studied extensively by several authors. Both permeability and infiltration of concrete are the most important hydraulic properties influencing the long-term durability of a concrete structure. While water head determinates the water flow in permeability; capillary forces play the most important role in infiltration. Likewise, these hydraulic properties depend on size and number of internal pores, micro cracks and capillaries that may also have an influence on thermal diffusivity [12]. Capillary action is the ability of a substance to draw another substance into it. Capillaries are formed during the curing process along with the evaporation of the excess water from the concrete surface. Understanding the quantitative relationship between the effective thermal conductivity and the moisture content is required to properly investigate the envelope heat and mass transfer and subsequently the building energy consumption [13] [14].

Considering the fact that the low permeable concrete structures will be strong and durable, nanomaterials are highly recommended for energy retrofitting and strengthening of existing structures. Some researchers have reported that Nanosilica (NS) and Silica fume (SF) might contribute to a decrement in the thermal conductivity of cement-based composites (concretes, mortars, and pastes), however, the trend reverses as a higher amount of additive is incorporated.

In order to investigate the effect of nano-structured materials on time-dependent thermophysical properties of concrete (*i.e.* the mechanical properties, permeability and thermal resistance), three types of nanoparticles including Zinc Oxide (ZnO), Magnesium Oxide (MgO), and composite nanoparticles were used in the present study as a partial replacement of cement.

2. Literature Review: The Typical Properties of Zinc Oxide and Magnesium Oxide Nanoparticle

In recent years, research on Zinc oxide nanoparticles (ZnO) and Magnesium oxide (MgO) nanoparticles as one of the prominent materials in thermal-oxide family have been increased. Zinc oxide nanostructures were prepared by thermal oxidation of Zn nanoparticles in air. Unique structure and mechanical properties of zinc oxide nanostructures as well as the simplicity of its production have made its usage more relevant. Due to its distinct physical and chemical proper-

ties, Zinc oxide has the great potentials in a wide range of applications, such as construction industries, textile industries, electronics and electro technology industries etc. However, very little information is available in the literature regarding the effects of ZnO nanoparticles on the performance of cement-based materials. It was reported that the mechanical strengths increased in mixtures containing MgO nanoparticles, nano-MgO behaved as a filler to enhance cement-based composites [15] [16] internal structure. Nanoparticles are characterized by various techniques such as powder X-ray diffraction (XRD), Scanning Electron Microscopy (SEM), Transmission electron microscopy (TEM), UV Visible spectrum, and etc. X-ray diffraction (XRD) as a rapid analytical technique is widely used for the crystalline phase identification in the nanostructured material and can provide information on average particles dimension, pore size investigation and atomic spacing. Partial replacement of Nano-Zinc oxide accelerates C-S-H gel formation at early stage of hydration, make more $Ca(OH)_2$. Some researchers showed by X-ray diffraction (XRD) analysis that Calcium zinc hydrate is formed with Nano-zinc oxide. In addition, Transmission electron microscopy (TEM) is commonly used to obtain the size of small nanoparticles through imaging, assess the shape and phase/crystallographic orientation information through a diffraction pattern and discovering chemical composition by means of the energy spectrum. TEM can produce very high-resolution images of a particle surface, revealing details about less than 1nm in size [17] [18]. The prepared Nanoparticles was characterized using Transmission Electron Microscopy (TEM) And X-Ray Diffraction (XRD). The physical and chemical properties of the nanoparticles used in this study are shown in **Table 1** and **Figure 2**.

Figure 2(c) and **Figure 2(d)** shows the Transmission electron microscopy (TEM) image under higher magnification of Zinc oxide (ZnO) and Magnesium oxide (MgO) in the nanometer scale. The XRD patterns of the nanoparticles recorded by using a powder X-ray (**Figure 2(e)** and **Figure 2(f)**) demonstrates the broadenings of the peaks due to crystallites with a diffraction angle between (10˚ - 70˚) and (30˚ - 90˚) in ZnO and MgO nanoparticles, respectively. The peaks are very sharp due to the nanocrystalline nature of the synthesized materials. The average size of nanoparticles was calculated using the Scherrer formula, which has been found to be 50 nm, and 20 nm for Zinc oxide and Magnesium nanoparticles, respectively.

Table 1. Physical and chemical specifications of ZnO, and MgO nanoparticles.

Component	Nano particle Size	Special surface	Purity (%)	Bulk density	Appearance
ZnO	50 nm	90 m^2/gr	99%	0.65 gr/m^3	White powder
MgO	20 nm	>60 m^2/gr	98%	0.145 gr/m^3	White powder

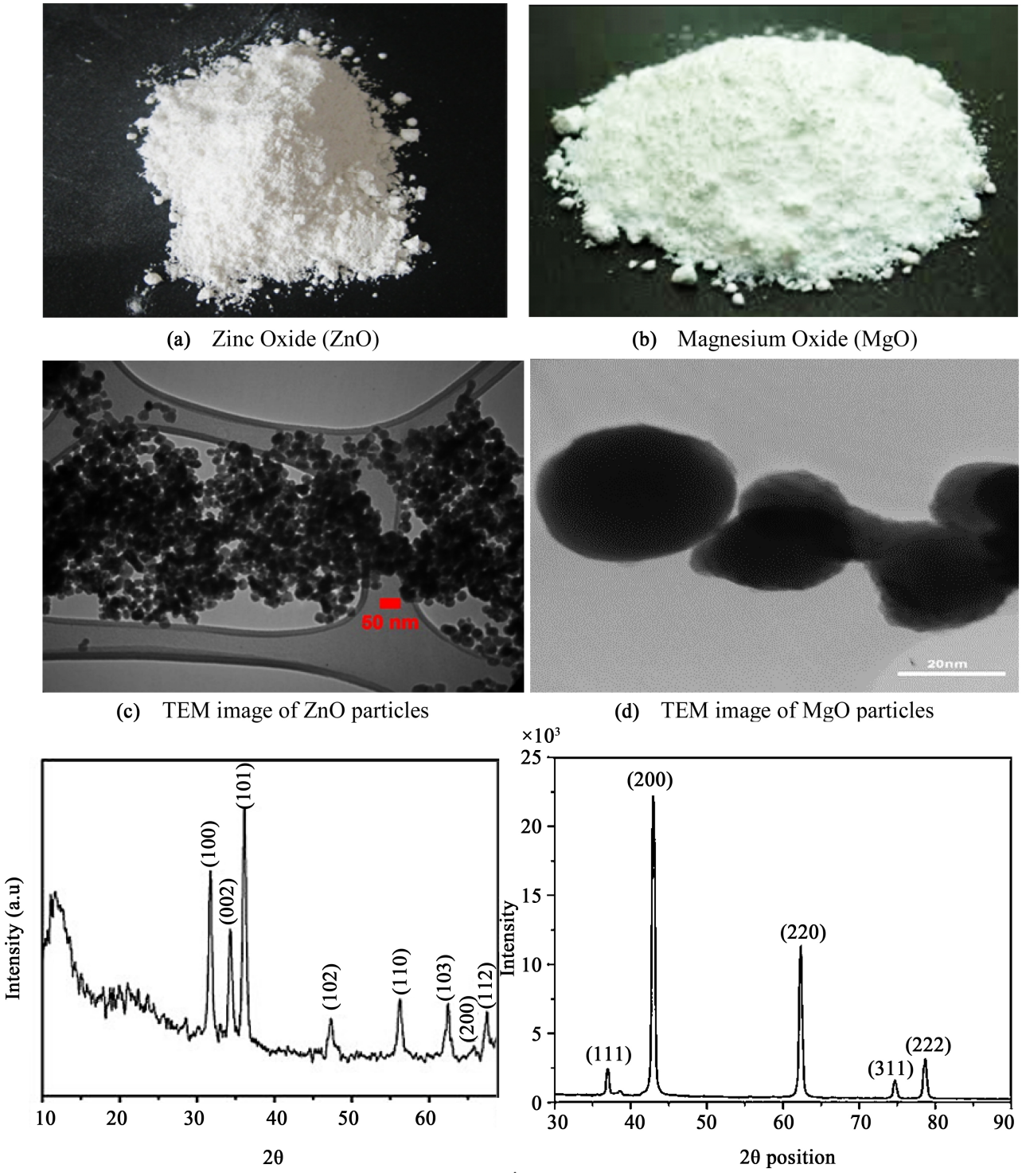

Figure 2. Crystalline phase characterization of ZnO and MgO nanostructured particles.

3. Homogeneous Distribution of Nano Materials

One major problem in the practical application of higher dosages of nanostructured materials is improper and poor distribution of nanoparticles within cement matrix (*i.e.* mortar and concrete), so-called pile-up effect phenomenon.

Due to volumetric changes associated with drying, nanoparticles tend to agglomerate and become a mass that produces weak-zones in the cement paste, mortar, and concrete, which suppress further increments in the mechanical strengths.

To achieve homogeneous dispersion of nano-materials within the cement matrix, nanomaterials should be initially poured in water, and then adding cement to the mixture, and set to 5 minutes in the ultrasonic device to mix. Figure 3 Shows the schematic picture of how nanoparticles distribution in cement mortar and concrete specimens.

The improvement of both mechanical properties and durability of nano blended concretes attained in case of well-dispersed nanoparticles has been found to be much higher than that proposed using empirical equations. There are several reasons for the occurrence of this fact: one is the decrease of the cement porosity and the total pore volume, along with improvement of its microstructure. The increase in the amount of high stiffness C-S-H phases in presence of well-dispersed nanoparticles, as revealed from the nanoindentation tests, is another reason for mechanical property enhancements in such cases. Extensive research techniques are available on literature which can be used for nanomaterial dispersion in cementitious matrix and resulting improvement in microstructure and mechanical properties.

For instance, to ensure proper and homogeneous distribution of nanoparticles in a cement matrix, Scanning Electron Microscopy (SEM) images of fractured surfaces can be effectively used. The following Figure 4 and Figure 5 demonstrate the SEM images taken from a failure surface of concrete specimens containing 0.5% ZnO, and 0.5% MgO nanoparticles, respectively. Using ultrasonic waves in concrete specimens, it will be obvious that the nanoparticles are well-dispersed in the cement matrix.

4. Methodology: Materials and Testing

The cement used in all samples was ordinary Portland cement (PC) equivalent to ASTM Type II, which the chemical characteristics, mineral composition, and some physical properties of it are shown in Tables 2-4. The specific gravity of cement was 3.13 and the initial setting time was 154 min. at 23.8 percent water for standard consistency. The water utilized was clean, free from impurities, and

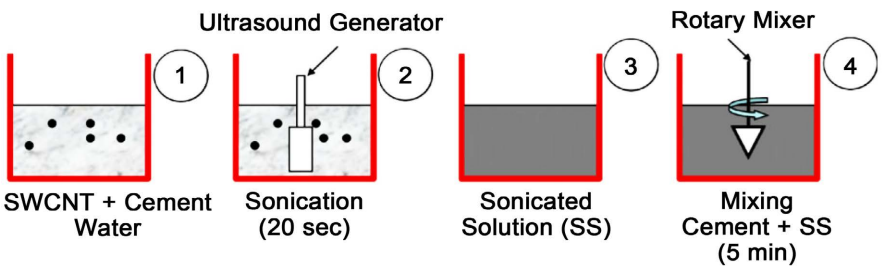

Figure 3. Nano particles dispersion in cement mortar matrix.

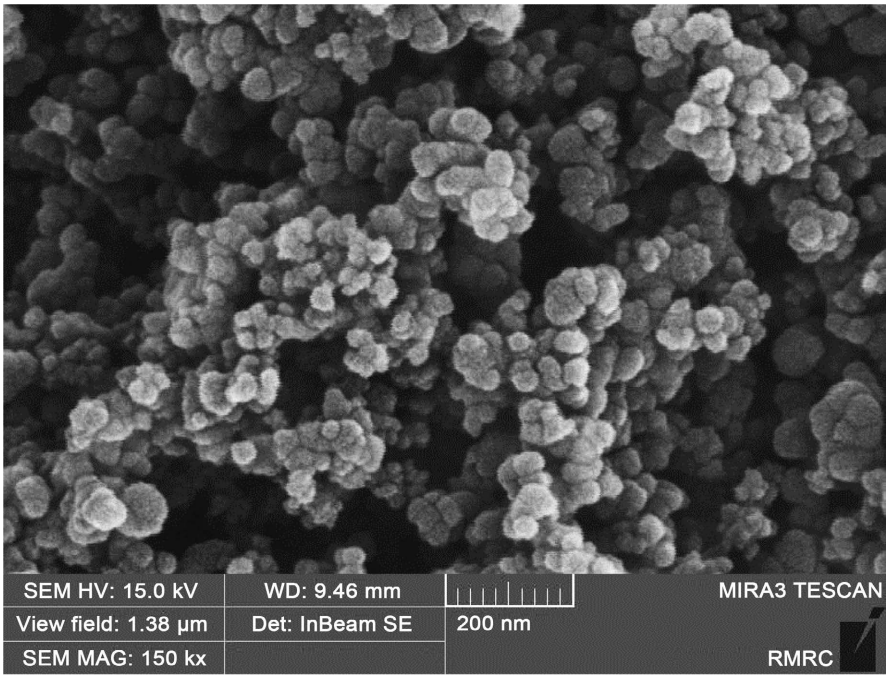

Figure 4. SEM image of a failure surface of concrete specimen, containing 0.5% ZnO nanoparticles.

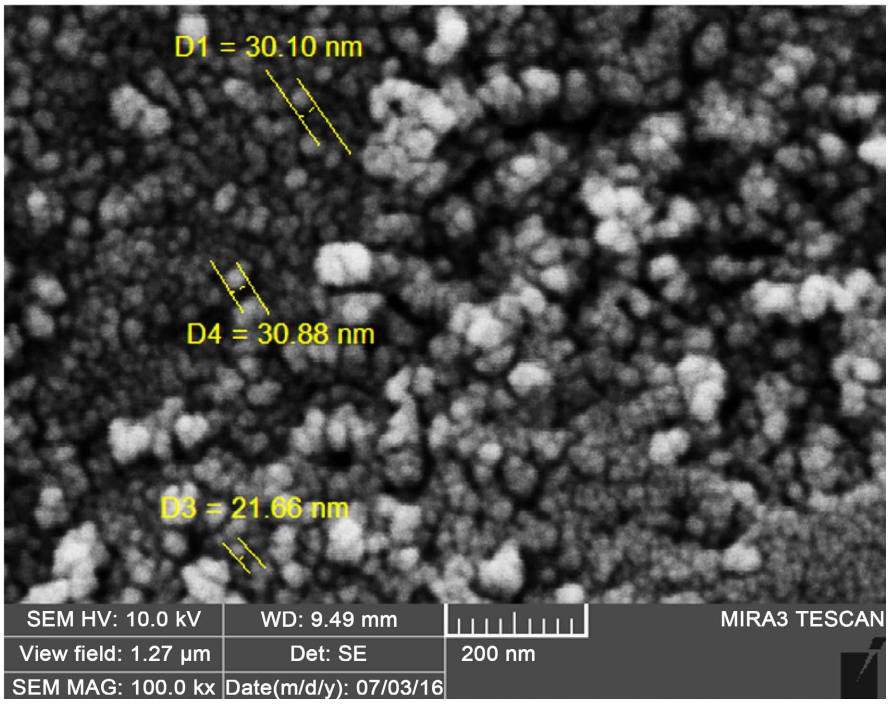

Figure 5. SEM image of a failure surface of concrete specimen, containing 0.5% MgO nanoparticles.

was taken from portable water supplies. Naphthalene sulfonate type superplasticizer, with the density of 1.2 m^2/kg and amount of 0.5 - 1.5 percent was also added (according to ASTM C494 [19] [20]) to the mix to improve workability.

Table 2. Chemical characteristics of the utilized Portland Cement (PC) in comparison with standard cement.

Cement Oxides	Percent of oxides		Comparison with standard cement
	Portland Cement (PC)	Standard Cement	
CaO	64.59	63 - 66	acceptable
SiO_2	22.05	20 - 22	acceptable
Al_2O_3	5.04	5.5 - 7.5	acceptable
Fe_2O_3	3.47	3 - 4.5	acceptable
SO_3	1.73	1 - 3	acceptable

Table 3. Mineral composition of the utilized Portland cement.

C_3S	C_2S	C_3A	C_4AF	C_3O
48.48	26.65	7.49	10.55	1.23

Table 4. Some physical properties of the utilized Portland Cement ("Sufian" Cement Co.).

Specific surface area (Blaine) cm^2/gr	Time of setting (minutes)		Water Content* (%) (According to ASTM C187)
	Initial	Final	
3049	154	181	23.8

*Amount of water required for normal consistency of cement.

In this investigation, crushed limestone aggregate with maximum size of 19 mm, specific gravity of 2.69 gr/cm^3, and 0.65% water absorption; and river sand with fineness modulus of 3.12, specific gravity of 2.81 gr/cm^3, and 0.9% water absorption were used as coarse and fine aggregates, respectively.

Thirteen concrete mix designs including base concrete (Control mixture) and nanoparticle blended concrete mixtures by adding three types of nanoparticles with different proportions of 0.1%, 0.5%, 1%, and 1.5% as a partial replacement of cement were prepared in accordance with ACI 211 [21] (Recommended Practice for Proportioning Normal and Heavy-weight Concrete Mixtures). The water per cementitious material ratio was held constant (w/cm = 0.61), and quantities of cement was about 350 (kg/m^3) for all the mixtures. **Table 5** shows the mixture proportions of the concrete mixes used in this study.

Concrete samples for mechanical tests were prepared in accordance with ASTM C192 and then were evaluated through a set of well-known experimental procedures. Compressive strength tests were carried out on fourteen 100 mm cubes in accordance with BS1881, and Brazilian splitting tensile strength tests were performed on fourteen 150 × 300 mm cylinders, according to ASTM C496. Average of at least three specimens made from the same concrete sample was reported for each mechanical test at ages of 7, 14, and 28 days. It should be noted

Table 5. Mixture proportions of the utilized base concrete and nanoparticle blended concretes.

Sample Code	Description	w/cm	Quantities (kg·m^{-3})				
			Nano Material (Kg/m^3)	Cement (Kg/m^3)	Sand (Kg/m^3)	Gravel (Kg/m^3)	Water (Kg/m^3)
N	Base project	0.61	0	336	684	1155	205
D21	0.1% nano ZnO		0.35	335.65	684	1155	205
D22	0.5% nano ZnO		1.75	334.25	684	1155	205
D23	1% nano ZnO		3.5	332.50	684	1155	205
D24	1.5% nano ZnO		5.25	330.75	684	1155	205
E21	0.1% nano MgO		0.35	335.65	684	1155	205
E22	0.5% nano MgO		1.75	334.25	684	1155	205
E23	1% nano MgO		3.5	332.50	684	1155	205
E24	1.5% nano MgO		5.25	330.75	684	1155	205
F21	0.1% NC		0.35	335.65	684	1155	205
F22	0.5% NC		1.75	334.25	684	1155	205
F23	1% NC		3.5	332.50	684	1155	205
F24	1.5% NC		5.25	330.75	684	1155	205

*NC: Nano-Composite.

that all test samples were subjected to the same temperature between 18˚C and 22˚C (normal room temperature), during tests. The mechanical test setups, and the compressive test specimen cube after failure is presented in **Figure 6**, which reveals Semi-explosive failure according to (BS EN 12390-3: 2002; Neville and Brooks, 2010).

To determine the water permeability and water absorption capacity of concrete samples at age of 28-days, both of these durability tests were conducted in accordance with DIN 1048-5 and ASTM C642, respectively. It has been demonstrated by many investigators that steady state flow conditions could not be achieved in concrete samples having low permeability even after subjecting the samples to pressures as high as 3.5 MPa for a test period extending up to several weeks.

For this test, the water is introduced on the top of the cell and the pressure of 0.5 N/mm^2 is applied in way to force the water to penetrate through the concrete sample. The measurement of the permeability is carried out by a method based on water penetration depth after 96 hrs. Water with a color indicator is used, which helps to determine the border of penetration depth. To measure the water coefficient by penetration, Valenta's law can be applied if the material is less permeable.

Figure 6. (a) The splitting tensile strength test setup, (b) The compressive strength test setup, (c) The compressive test specimen cube after failure (Semi-explosive failure).

$$k = \frac{D^2 V}{2HT}$$

where, k = Water permeability coefficient (m/s), D = depth of penetration (m), V = Volume of voids filled by water in the penetrated zone, H = Applied pressure (1 bar = 10 m), and T = Time to penetrate to depth D (s).

5. Research Results

Figures 7-10 clearly show the mechanical strength of nanoconcrete specimens after 7 and 28 days of curing as a function of nanoparticles replacement percentage. In these diagrams, the horizontal axis presents the percentage of ZnO, MnO, and Composite nanoparticles as partial replacement of cement, and the vertical axis shows the mean Compressive/Tensile strength of three samples obtained in kg/cm^2. Details of the mean compressive strengths and tensile strengths are given in Table 6 and Table 7, respectively.

The mean of the maximum depth of penetration and amount of water absorption from three concrete specimens tested were taken as the test result, as shown in Table 8. Permeability ranges according to standard DIN 1048 (Part 5) are reported in Table 9.

1) According to the results obtained, the optimal replacement of Zinc oxide nanoparticles used in the project was 1%.

2) Experiments show that fluidity of cement sand mortar and concrete samples containing nanoparticles decreased. This can be due to the size of the nanoparticles, so they absorb more water and dry the mixture.

3) The optimum replacement percentage of nanoparticles used in the project was determined as follows:

4) Experiments show that the Fluency of cement sand mortar and concrete samples containing nanoparticles decrease. The reason for this can be traced to the fineness of the nanoparticles and more water absorption of it, which causes the mixture to dry.

5) As can be seen from the results of the experiments, of the three types of nanostructures used in the project, the composite of nano-oxide-magnesium and nano-oxide had more favorable effects on the mechanical strengths of the cement

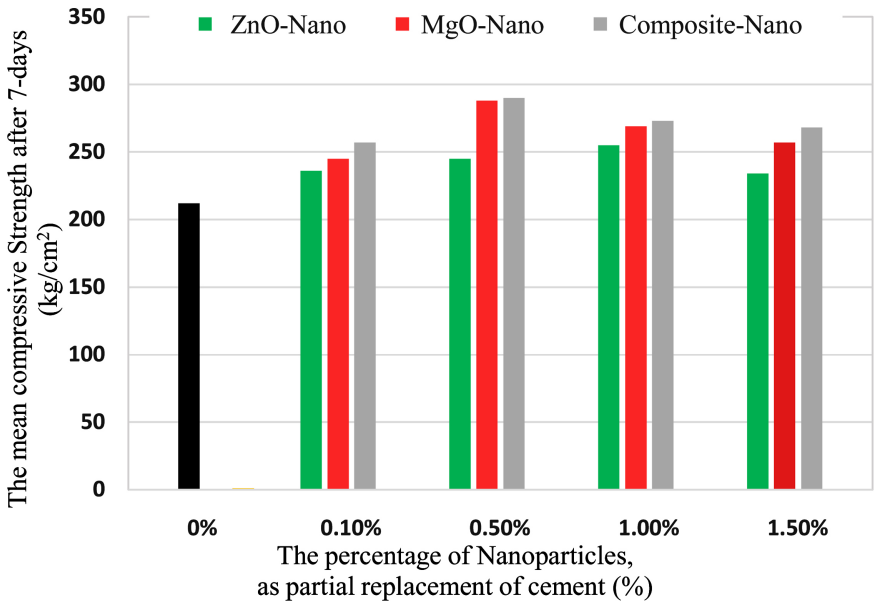

Figure 7. The mean compressive strength of concrete specimens after 7-days.

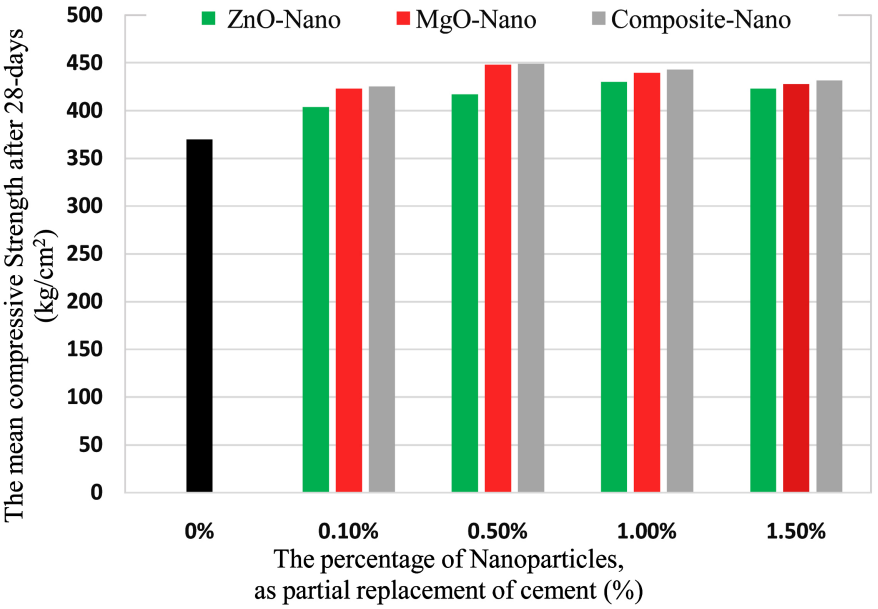

Figure 8. The mean compressive strength of concrete specimens after 28-days.

mortars and concrete samples than the oxide-only nanoparticles and the magnesium oxide nanoparticles.

6) Experiments show that the Fluency of cement sand mortar and concrete samples containing nanoparticles decrease. The reason for this can be traced to the fineness of the nanoparticles and more water absorption of it, which causes the mixture to dry.

7) As can be seen from the results of the experiments, of the three types of nanostructures used in the project, the composite of nano-oxide-magnesium and

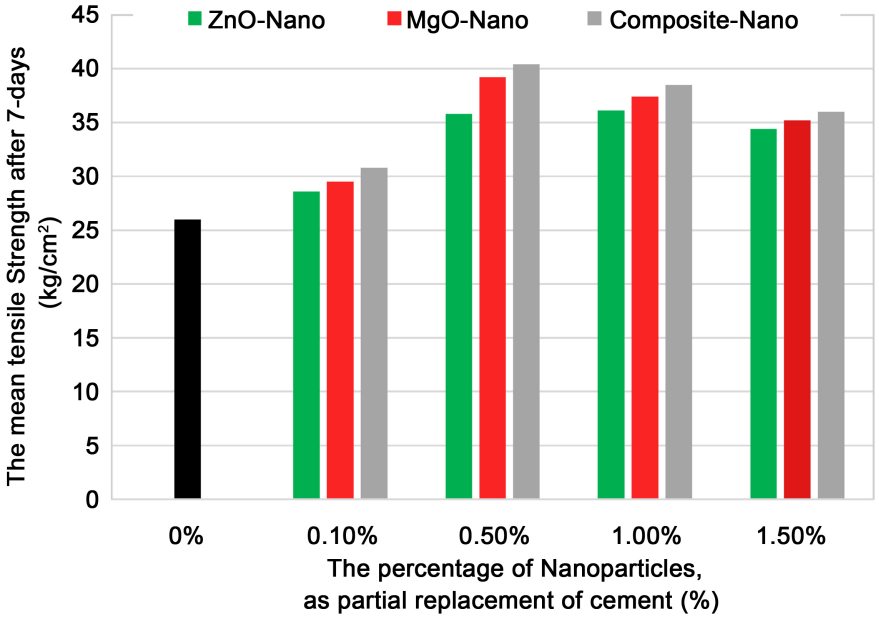

Figure 9. The mean tensile strength of concrete specimens after 7-days.

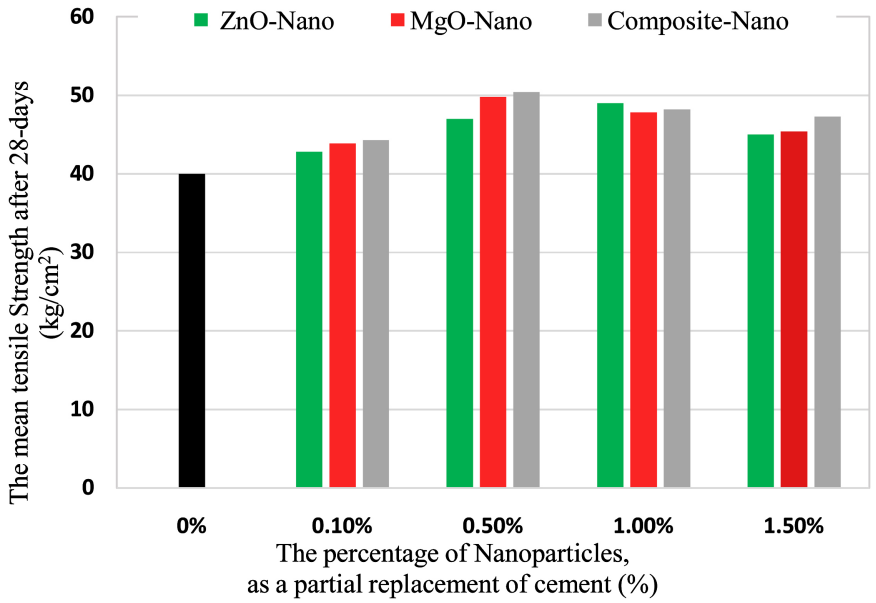

Figure 10. The mean tensile strength of concrete specimens after 28-days.

nano-oxide had more favorable effects on the mechanical strengths of the cement mortars and concrete samples than the oxide-only nanoparticles and the magnesium oxide nanoparticles, the optimal percentage of nanoparticles are shown in Table 10.

6. Numerical Simulation (Genetic Programming)

There are various types of numerical approaches which has been proposed by investigators in recent years to predicted the mechanical strengths of cementations

Table 6. The mean compressive strength of concrete specimens (kg/cm^2).

Sample code	7 days	14 days	28 days
N	212	305	370
D21	236	335	403.7
D22	245	345	417.2
D23	255	355	430
D24	234	350	423.1
E21	245	350	423
E22	288	370	447.9
E23	269	365	439.7
E24	257	355	428
F21	257	352	425
F22	290	372	449
F23	273	367	443
F24	268	359	431.6

Table 7. The mean tensile strength of concrete specimens (kg/cm^2).

Sample code	7 days	14 days	28 days
N	26	33	40
D21	28.6	35.5	42.8
D22	35.8	39.1	47
D23	36.1	40.2	49
D24	34.4	37.4	45
E21	29.5	36.5	43.9
E22	39.2	41.3	49.8
E23	37.4	39.7	47.8
E24	35.2	37.7	45.4
F21	30.8	36.8	44.3
F22	40.4	41.8	50.4
F23	38.5	40.1	48.2
F24	36	39.4	47.3

materials such as regression analysis methods, artificial neural network (ANN), support vector machine (SVM), genetic programming method (GP), fuzzy logic (FL), and adaptive neurofuzzy inference system (ANFIS) [22] [23] [24]. The great advantage of GP method among these well-known algorithms is the capability of it to provide practical prediction equations, which makes it an alternative

Table 8. Water permeability and Water absorption of concrete specimens.

Sample code	Water Permeability (mm) *Depth of water penetration	Water Absorption (%)
N	55	3.995
D21	45	3.78
D22	41	3.42
D23	37	3.06
D24	32	2.60
E21	35	4.08
E22	30	3.52
E23	28	3.30
E24	21	2.53
F21	40	3.90
F22	36	3.50
F23	32	3.11
F24	25	2.42

Table 9. Permeability ranges according to standard DIN 1048 (Part 5).

Permeability as per to DIN 1048 standard	Low	Medium	High
Penetration depth after 96 hrs.	Less than 30 mm	30 - 60 mm	Greater than 60 mm

Table 10. Optimal percentage of nanoparticle replacement.

Type of nano particle	Nanocomposite	Magnesium nano oxide	Zinc nano oxide
Optimal percentage	0.5%	0.5%	1%

approach. Considering a large number of factors affecting the mechanical behavior of cementitious materials and reduction of test samples, Genetic Programming (GP) can be utilized as an effective tool for identifying non-linear patterns along with predicting mechanical properties. Genetic Programming (GP) generates simplified prediction equations without assuming prior form of the existing relationship. In this study, we propose a new multigene genetic programming (MGGP) approach to derive prediction models for the mechanical strengths of nano blended concretes. For this purpose, we use the multi-tree representation to match with the existing experimental results. The mixture proportions (*i.e.*, amount of Fine aggregates/Coarse aggregates, Cement, Water

content, Type of nanoparticle and its percentage) and the concrete age were considered as influencing features. The compressive strengths and tensile strengths of specimens were separately used to derive two different MGGP-based formulas for each kind of the nano blended concretes. The input variable FT is used to identify the type of nanoparticle component, which is taken as 0 (for Control mixture-without NP), 1 (for mixtures containing ZnO particles), 2 (for mixtures containing MgO particles) and 3 (for mixtures containing composite particles). As shown in the table, due to the random nature of the proposed algorithm, ten independent executions (runs) were performed, finally the best relation has been reported. More particularly, for each run 70% of the observations were selected at random with uniform distribution to form the training set, while the remaining 30% form the test set.

A fairly large number of generations are tested to find models with minimum error. The GP parameters used in our experiments are summarized in Table 11. To evaluate the model results, it is necessary to set criteria to assess the performance and accuracy of the model prediction. Therefore, the optimum pattern is selected based on the following criteria:

The first criterion is the simplicity of the model, which is controlled by the user by adjusting the tree depth parameters as well as simple mathematical functions. On the other hand, there are many static parameters to determine the best fitness value on the entire data, including Root Mean Squared Error (RMSE), Mean Absolute Error (MAE), Mean Absolute Percentage Error (MAPE), Pearson correlation coefficient (R) and OBJ, which are used to evaluate the performance of the models. These parameters are calculated using the following equations:

Table 11. GP parameters used in our experiments.

Parameter	value
Number of generations	200
Number of population members (chromosomes)	50
Depth of tree	5
Depth of mutation	4
selection method	competitive
Percentage of elitism	5
Intersection percentage	85
Percentage of mutation	10
Functions used	Addition, subtraction, multiplication, division
Fixed numbers	[−1, 1]
Number of iterations	10

$$\mathrm{MAE} = \frac{\sum_{i=1}^{n} |h_i - t_i|}{n}$$

$$\mathrm{MAPE} = \frac{1}{n} \sum_{i=1}^{n} \frac{|h_i - t_i|}{t_i} \times 100$$

$$R = \frac{\sum_{i=1}^{n} \left(h_i - \overline{h_i}\right)\left(t_i - \overline{t_i}\right)}{\sqrt{\sum_{i=1}^{n} \left(h_i - \overline{h_i}\right)^2 \sum_{i=1}^{n} \left(t_i - \overline{t_i}\right)^2}}$$

$$\mathrm{OBJ} = \left(\frac{\mathrm{No.}_{\mathrm{Train}} - \mathrm{No.}_{\mathrm{Test}}}{\mathrm{No.}_{\mathrm{Train}} + \mathrm{No.}_{\mathrm{Test}}}\right) \frac{\mathrm{RMSE}_{\mathrm{Train}} + \mathrm{MAE}_{\mathrm{Train}}}{R_{\mathrm{Train}} + 1} + \frac{2\mathrm{No.}_{\mathrm{Test}}}{\mathrm{No.}_{\mathrm{Train}} + \mathrm{No.}_{\mathrm{Test}}} \times \frac{\mathrm{RMSE}_{\mathrm{Test}} + \mathrm{MAE}_{\mathrm{Test}}}{R_{\mathrm{Test}} + 1}$$

where, h_i and t_i are the actual and predicted outputs for i^{th} data, respectively. $\overline{h_i}$ and $\overline{t}$ are the practical and predicted average outputs, respectively. Besides, n, $\mathrm{NO.}_{\mathrm{Train}}$ and $\mathrm{NO.}_{\mathrm{Test}}$ are the total number of samples in dataset, training data, and test data, respectively.

6.1. Predicted Model for Compressive Strength of Nano-Concretes

Using Genetic Programming algorithm, a set of runs has been performed in MATLAB software to find the best tuning of parameters for the compressive strength results, and finally the optimum pattern was selected.

The diagrams of the variations of the statistical parameters of the results of the training and test errors with the number of generations are shown in Figure 11. As expected, the performance of the algorithm improves with increasing the number of generations.

The function of the compressive strength of nano-concretes represented by a tree-structure, as demonstrated in Figure 12. Each subtree represents a complete derivation for the label of its root node. The parameters used in this equation are

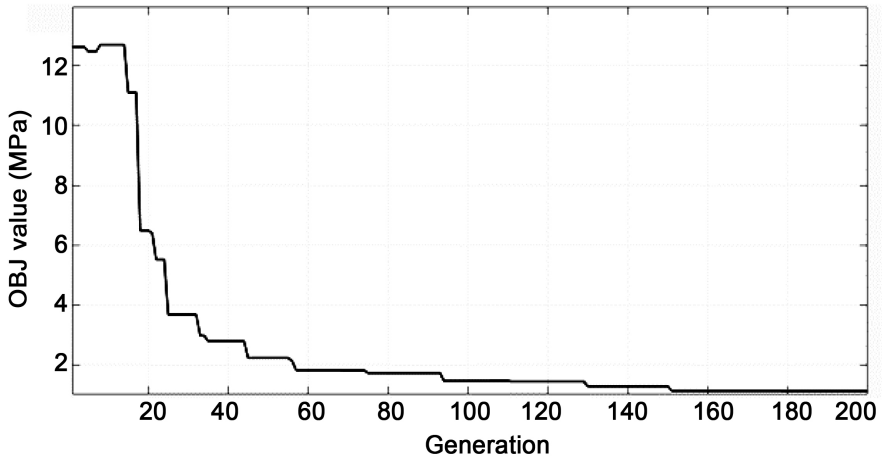

Figure 11. Statistical parameter related to the compressive strength model of nano-concrete.

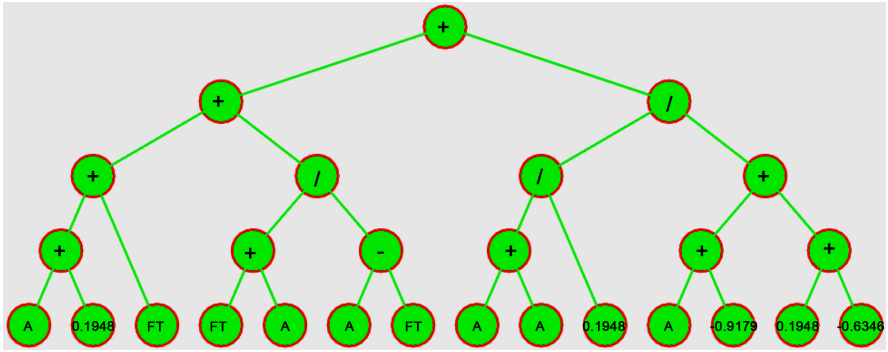

Figure 12. The final tree structure of the compressive strength model for experimented nano-concretes.

"FT" and "A", which represent the type of nano-fibers and the concrete age, respectively.

The distribution function is used to distribute semantic constraints among the tree roots. Based on the evaluation of the tree-structure, the compressive strength of nano-concretes can be calculated as follows:

$$f_c' = A + FT + \frac{A + FT}{A - FT} + \frac{2A}{0.1948A - 0.2645} + 0.1948$$

As can be seen from this equation, the fiber content had no significant effect on the compressive strength of the concrete with the nano-fibers as it was omitted from the proposed equation. The statistical parameters of the proposed model are presented in the table below. As shown in Table 12, there is a good correlation (0.9837 for training data and 0.9990 for test data) between the results of the model and the experimental results, which confirms the accuracy of the model. Moreover, the error rate of the proposed model for all data sets is equal to 3.5061%.

In Figure 13, the three-dimensional sensitivity analysis displays the compressive strength of nano-concretes based on the fiber type (FT) and the concrete age (A). As expected, with increasing the age of concrete, the compressive strength of nano-concretes increased and effect of aging was much higher than the type of nanofibers. With respect to the impact of the type of nanoparticles on the compressive strength values, it can be observed that magnesium oxide was much more effective than zinc oxide in terms of enhancement in the compressive strength of nano-concretes.

6.2. The Predicted Model for the Tensile Strength of Nano-Concretes

To determine the tensile strength of concrete containing nano-particles, the compressive strength of concrete, amount, and type of the nano-fibers were considered as the inputs of the model. Using Genetic Programming algorithm, a set of runs has been performed in MATLAB software to find the best tuning of parameters for the tensile strength results, and finally the optimum pattern was

Table 12. Values of static parameters of nano fiber concrete compressive strength model.

	RMSE (MPa)	MAE (MPa)	MAPE (%)	R	OBJ (MPa)
Training data	1.5868	1.2402	3.9494	0.9837	
Test data	0.9064	0.7016	2.0285	0.9990	1.1387
Total data	1.4582	1.1159	3.5061	0.9869	

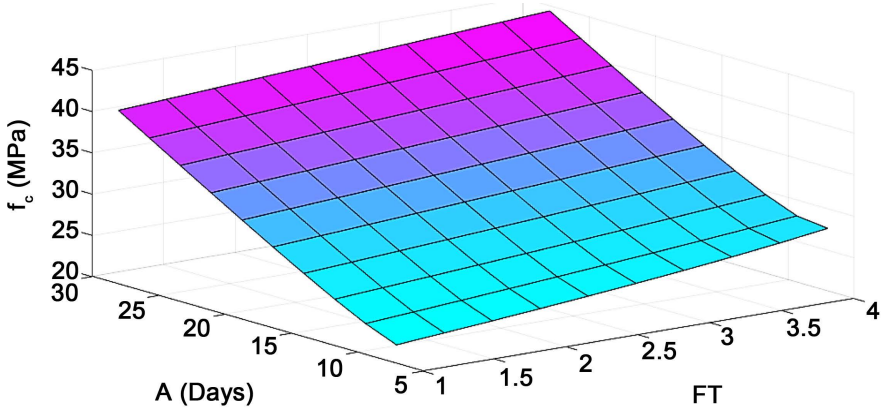

Figure 13. The three-dimensional relationship between the compressive strength (f_c'), FT (Type of nano fibers, and A (concrete age).

selected. Similar to the previous section, the performance of the algorithm improves with increasing the number of generations, see **Figure 14**.

The final tree-structure pattern for tensile strength is generated, as shown in **Figure 15**. In this figure, f_c' and FC are the compressive strength of the concrete and the percentage of nano-fiber, respectively.

According to the parameterized derivation tree, the tensile strength of nano-concretes can be estimated by the following equation:

$$f_t = \sqrt{f_c'} - \sqrt[3]{\sqrt{f_c'} - \sqrt{FC}}$$

In this respect, the type of nano-fibers used did not have a significant effect on the tensile strength of concrete containing nano-fibers in comparison with other factors, accordingly it was automatically removed from the proposed relationship.

The values of the statistical parameters in the proposed model are given as follows. As shown in **Table 13**, there is a good correlation (amount of 0.9573 for training data and 0.9170 for test data) between the predicted results and the experimental results. Besides, the average error of the proposed model is 0.1933 MPa for the whole data set.

The **Figure 16** shows the three-dimensional sensitivity analysis of tensile strength of nano-fiber concrete based on fiber content in percentage (FC) and compressive strength of concrete (f_c'). As expected, as the compressive strength of the concrete rises, the tensile strength of the concrete increases, and this

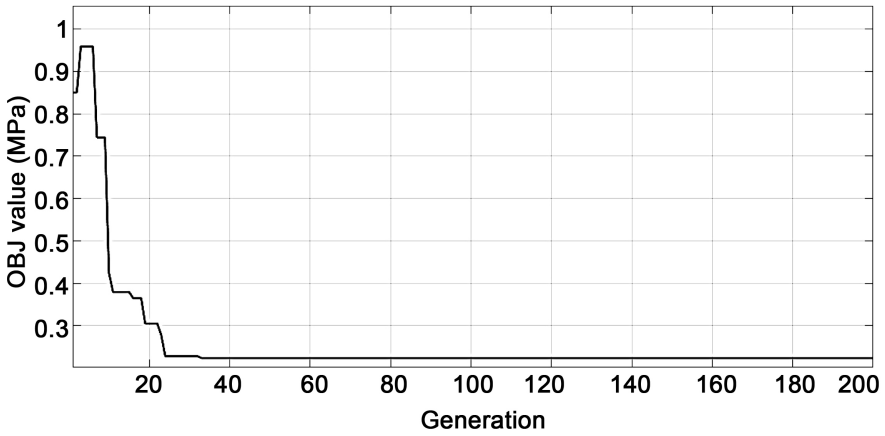

Figure 14. Statistical parameters related to the tensile strength model of nano-concrete.

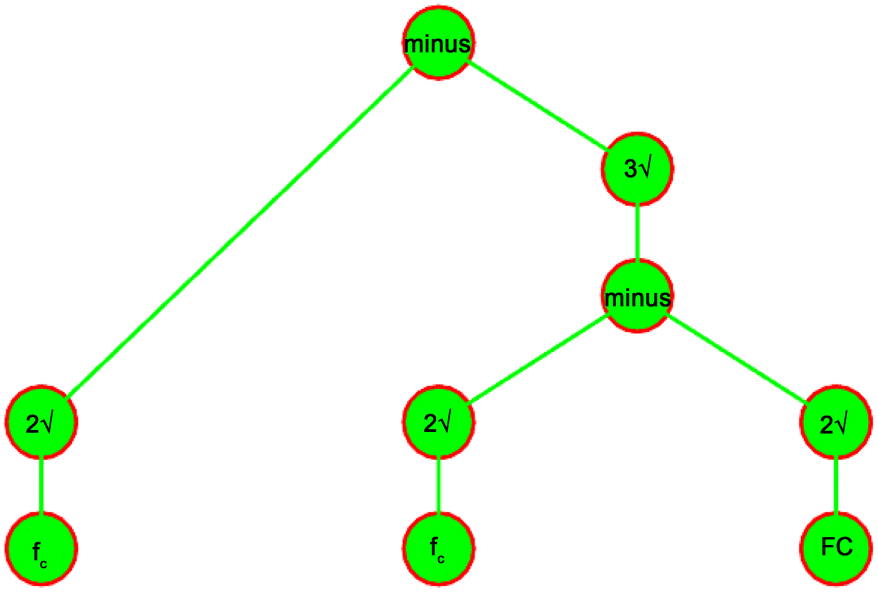

Figure 15. The final tree structure of the tensile strength model for experimented nano-concretes.

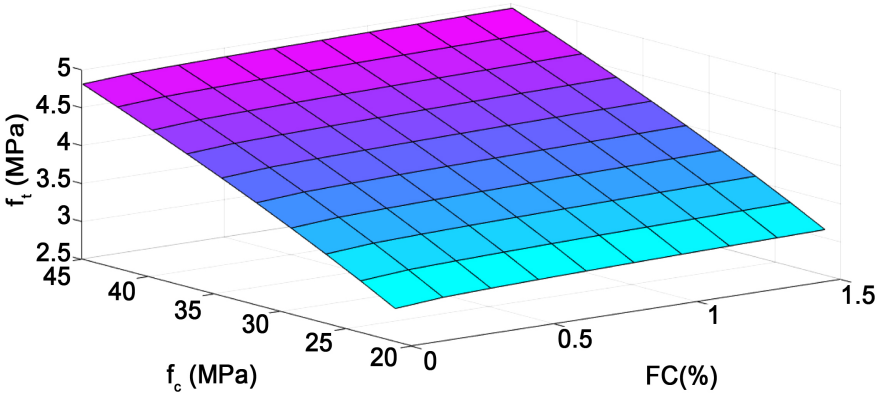

Figure 16. The three-dimensional relationship between the tensile strength (ft), FT (Type of nano fibers, and A (concrete age).

Table 13. Static parameter values of the relationship between the tensile strength of concrete and nano-fibers.

	RMSE (MPa)	MAE (MPa)	MAPE (%)	R	OBJ (MPa)
Training data	0.2097	0.1823	4.7198	0.9573	
Test data	0.2511	0.2299	6.1128	0.9170	0.2237
Total data	0.2199	0.1933	5.0413	0.9507	

increased rate is higher than the effect of the amount of fiber in the concrete. By increasing the amount of concrete fiber in the mixing design, the tensile strength is also significantly increased.

7. Discussion and Analysis

Concrete mechanical properties improve mechanisms using nanoparticles can be stated as follows:

1) Considering the microstructure of concrete and the existence of pores in the nanometer scale, the use of nanoparticles can fill the gaps and pores even the ones on the nanometer scale and make the concrete structure denser, resulting in the increase of mechanical strength, including compressive and tensile strength.

2) Nanoparticles react with calcium hydroxide ($CaOH_2$) and prevent the overgrowth of these crystals. As a result of this reaction, a dense gel of C-S-H is produced, which makes the concrete structure denser and thus improve the mechanical properties of concrete.

3) Given the very high specific surface of nanoparticles, resulting in very high surface energy, nanoparticles act as the nucleus of an atom and strong adhesion with the hydrated cement forms, that the effect is called nucleation. As a result of this effect due to the high reactivity of nanoparticles, the hydration process continued and mechanical strength increased.

4) New properties in the concrete: In concrete, when the cement is poured water and the reaction begins, the reactions that take place (between the different phases of cement with water) are in the nanometer scale. If the nanomaterials were to be added to this collection, it becomes much more complex, and the concrete gets special properties. For example, the use of additives such as micro-silica causes longer life and durability of concrete increases. If these add-ons can be used in the nanometer scale, properties improve.

Of course, the use of nanoparticles in concrete can have negative effects, too. May be due to poor distribution of nanoparticles in the mixture, a mass of nanoparticles in coming, and they form the cavities in the cement paste, thereby reducing the resistance. For optimum distribution of nanoparticles in the concrete mix, there are two methods: The use of surfactants with the trade name of SFC and the use of ultrasonic waves. Another negative effect of the nanoparticles occurs when water to cement ratio is higher. Nanoparticles having microscopic

dimensions, absorb more water, resulting mixture to be dry, thus causing high water to cement ratio in concrete. Super-plasticizer is used to solve this problem.

It can be observed that with increasing in the amount of nanoparticles to a certain extent, compressive and tensile strength of concrete and cement-sand mortar samples increases. As seen in the charts, replacing the high percentage of nanoparticles have adversely affect the structure and mechanical properties of mortar and concrete instead of the desired effect on mechanical properties of concrete. This can be due to their high specific surface, which causes the surface energy of nano particles to be higher. This creates a low resistance of pores in the concrete of the structure, thus causes the structure to appear dense, but is loose. Table 14 show the percent increase in mechanical strength of samples made with nanomaterials compared to control samples.

8. Nano Insulating Materials for Energy Retrofit of RC and Masonry Buildings

In order to achieve the energy efficiency targets set by the European Union (EU), there is a growing tendency towards the use of innovative insulation materials which are able to provide high levels of thermal protection in construction sector.

Among different classes of materials, nanotechnological insulation materials and smart materials like phase change materials (PCM) are the most widely used in building refurbishment projects due to their properties and their relatively simple and reliable preparation method. Following increased application of nanomaterials in a large variety of matrix materials, low density, high-performance

Table 14. Percentage increase in mechanical strength of concrete samples made with nanomaterials compared to the plain concrete.

	Compressive Strength		Tensile Strength	
	7 Days	28 Days	7 Days	28 Days
D21	11%	9%	10%	7%
D22	15%	12%	37%	17%
D23	20%	16%	38%	22%
D24	10%	14%	32%	12%
E21	15%	14%	13%	9%
E22	35%	21%	50%	24%
E23	26%	18%	43%	19%
E24	21%	15%	35%	13%
F21	21%	14%	18%	10%
F22	36%	21%	55%	26%
F23	28%	19%	48%	20%
F24	26%	16%	38%	18%

composite aerogels have been developed for use in insulating layers. The aerogels are solid nanoporous materials with an exceptionally high porosity, which permits them to have a lower thermal conductivity than air (~0.01 - 0.02 W/mK). The main advantage of aerogel-enhanced products for energy retrofit of building is in their space saving benefit, since makes it a valid alternative with low thickness among the other traditional thermal-insulating products. Nanopores with diameters less than 100 nanometers occupy more than 90% of the total volume of the aerogel, whose bulk density often varies between 70 kg/m^3 and 150 kg/m^3. The aerogel is capable of operating in a temperature range between −200˚C and +650˚C; and effectively ensures thermal performance conservation regardless of operating temperature, whereas traditional insulating materials usually become more conductive as air temperature rises.

Despite being extremely brittle, its peculiar microstructure, with a specific surface area up to 800 m^2/g, gives aerogel compression strength able to bear a load of up to 4000 times its own weight. Table 15 reports the main properties of silica aerogels, the most common aerogel in construction applications.

Figure 17 illustrates the raw materials for aerogel-enhanced plaster and preparation process. Aerogel structure network is heavily crosslinked and full of dead-ends, helping in trapping air molecules inside. This way it is possible to block effectively heat transfer by convection. Moreover, aerogel-enhanced plasters have the benefit of being simple to implement and flexible with respect to unevenness surfaces allowing to create a continuous thermal insulation layer by filling the gaps and joints in a building envelope.

Table 15. The main physical properties of silica SiO_2 aerogels.

Property Density	Value
Density	3 - 350 kg/m^3 (typical 70 - 150 kg/m^3)
Pore diameter	1 - 100 nm (~20 nm on average)
Porosity	85% - 99.9% (typical ~95%)
Thermal conductivity	0.01 - 0.02 W/mK
Primary particle diameter	2 - 4 nm
Surface area	600 - 1000 m^2/g
Tensile Strength	16 kPa
Coef. Of linear expansion	$2.0 - 4.0 \times 10^{-6}$

Figure 17. The raw materials for aerogel-enhanced plaster and preparation process.

To improve the mechanical characteristics of aerogel products in order to ease its use in insulating opaque enclosures, aerogel is usually integrated in a PET fibrous support structure, obtaining Fiber Reinforced Aerogel Blankets (FRAB) such as Aspen Aerogels Spaceloft. The main aerogel insulating products are shown in Figure 18. Another application of FRABs is also in combination with Phase Change Materials for energy retrofitting of existing masonry or concrete walls by using interior insulation systems. By combining a PCM board with aerogel insulation, it is possible to obtain an insulated double wall with minimum thickness (2 - 3 cm), capable of reducing energy loss and at the same time of supporting heating systems, minimizing air temperature fluctuations and reducing overheating during summer. Using traditional materials with comparable performance would lead to an increase in wall thickness up to 30 cm.

The Swiss Federal Institute EMPA has developed a new insulating aerogel plaster together with Fixit AG, which is commercially available under the name of Fixit 222. This material is composed of more than 50% silica aerogel by volume and its thermal conductivity is nearly the same as that of in silica-aerogel (~0.028 W/(mK)). Aerogel holds 15 entries in the Guinness book of world records, including the one as the best Isolator. The main properties of the different aerogel-enhanced plasters are reported in Table 16.

With regard to the advances of nanotechnology in the field of materials science, the nanotechnology applications are constantly evolving, particularly in the case of grout injections for both energy efficiency and structural strength purposes in existing buildings. Nano-grout is injected into the wall through pipes placed in holes previously made in the masonry/concrete under moderate pressure (0.5 - 1.5 bar). In the experiments by Baltazar *et al.* the contribution of Silicafume and Nanosilica on the mechanical strength and durability of injection grouts were studied, focusing on the water absorption by capillarity in old stone masonry building. It was found that the use of Nanogrout materials could allow to significantly reduce the open porosity as well as the absorption of capillary water of existing walls while maintaining their integrity and architectural quality, in order to achieve the goals of reducing primary energy consumption in the

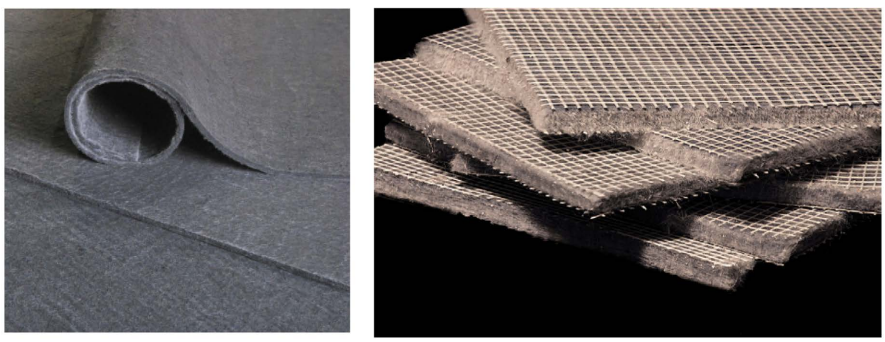

Figure 18. The main aerogel insulating products on the market: (a) Aspen Aerogels Spaceloft, (b) AMA Composites Aeropan Basic.

Table 16. The main properties of the different aerogel-enhanced plasters.

Mixture	Composition			Aerogel [vol.%]	Density [kg/m^3]	Thermal conductivity at 24˚C [W/(mK)]
	Plaster	Aerogel	Water			
Fixit 222	5.5	0	1.534	0	241.3	0.0323
Fixit 222 + 15% aerogel	4	0.8	1.355	15	203.8	0.0276
Fixit 222 + 5% aerogel	4	1.6	1.579	25	199.3	0.0275
Hydraulic lime	6	0	2.174	0	1109.8	0.2032
Hydraulic lime + 25% aerogel	5	2.5	2.7	25	735.6	0.1151
Hydraulic lime + 50% aerogel	2	3.5	1.26	50	501.0	0.0687
Hydraulic lime + 70% aerogel	0.4	1.5	0.3	70	260.7	0.0311
Saint Astier Plaster	6	0	1.5	0	1109.84	0.1906
Saint Astier + 25% aerogel	5	2.5	2.7	25	735.56	0.1231
Saint Astier + 50% aerogel	2	3.5	1.26	50	515.30	0.0694
Saint Astier + 70% aerogel	0.4	1.5	0.3	70	236.78	0.0306

*a Fixit 222 has a declared dry bulk density of 220 kg/m^3 and contains between 50% and 70% vol. of aerogel.

building sector. On the other hand, the influence of adding nano-based grouting materials on the structural strength development of cementitious materials was positive, increasing the compressive strength to an extent dependent on the Nanosilica content, w/b ratio and curing time. Using nanogrout insulation materials within the exterior side walls of the building allows to enhance the thermal capacity of walls and reduce temperature fluctuations throughout the day, while reconcile the needs for structural quality with the new requirements for energy efficiency.

In this context, Berardi selected Ryerson University building known as Monetary Times building located in Toronto as an exemplary building, to assess the practical efficiency and economical aspects of several energy retrofitting actions related to the building envelope in a cold climate, such as new aerogel-enhanced plasters, blankets, and glazing systems. The case study was located in an area with extremely high real estate values, thus the retrofit interventions had to include only thin, easy, and fast to install systems. Table 17 exhibits some retrofitting strategies with aerogel-enhanced products for the monetary building together with their practical impacts, cost aspects, and payback time. The economical analysis of these interventions was conducted based on Canadian contractors and supplied pricing. The thermal plaster application induced a significant reduction of the wall thermal transmittance, from 0.94 W/(m^2·K) to 0.65 W/(m^2·K), while adding aerogel blankets resulted in a thermal transmittance equal to 0.54 W/(m^2·K). The energy demand of the building with the adoption of aerogel-incorporating glazing systems, also resulted in a high primary cost due to the not competitive price of aerogel, with long payback period.

Table 17. Retrofitting strategies for the monetary building together with their impacts.

Mixture	Composition			Aerogel [vol.%]	Density [kg/m^3]	Thermal conductivity at 24˚C [W/(mK)]
	Plaster	Aerogel	Water			
Fixit 222	5.5	0	1.534	0	241.3	0.0323
Fixit 222 + 15% aerogel	4	0.8	1.355	15	203.8	0.0276
Fixit 222 + 5% aerogel	4	1.6	1.579	25	199.3	0.0275
Hydraulic lime	6	0	2.174	0	1109.8	0.2032
Hydraulic lime + 25% aerogel	5	2.5	2.7	25	735.6	0.1151
Hydraulic lime + 50% aerogel	2	3.5	1.26	50	501.0	0.0687
Hydraulic lime + 70% aerogel	0.4	1.5	0.3	70	260.7	0.0311
Saint Astier Plaster	6	0	1.5	0	1109.84	0.1906
Saint Astier + 25% aerogel	5	2.5	2.7	25	735.56	0.1231
Saint Astier + 50% aerogel	2	3.5	1.26	50	515.30	0.0694
Saint Astier + 70% aerogel	0.4	1.5	0.3	70	236.78	0.0306

It was revealed that high thermal resistance values can be achieved by installing thin aerogel-enhanced systems in the opaque and transparent envelope, while can bring up to a 34% savings in overall energy usage for a building, and limited impacts and interruptions on the building functionality and internal usable space.

9. Conclusions

The main conclusions drawn from the results are given as follows:

1) Considering the mechanical strength of mortar and concrete test results, with increasing amounts of nanoparticles replacing to a certain extent, nanomaterials create dense structure and low porosity in the mixed mortar and concrete, improving the mechanical strength.

2) Nano material's nanoscale filling effect:

Considering the microstructure of concrete and the existence of pores on the nanometer scale, the use of nanoparticles can fill the gaps and pores even the ones on the nanometer scale and make the concrete structure denser, resulting in the increase of mechanical strength, including compressive and tensile strength.

3) Nanoparticles react with calcium hydroxide ($CaOH_2$) and prevent the overgrowth of these crystals. As a result of this reaction, a dense gel of C-S-H is produced, which makes the concrete structure denser and thus improves the mechanical properties of concrete.

4) Nucleation effect:

Given the very high specific surface of nanoparticles, resulting in very high surface energy, nanoparticles act as the nucleus of an atom and have strong ad-

hesion with the hydrated cement forms, the effect is called nucleation. As a result of this effect due to the high reactivity of nanoparticles, the hydration process continued, and mechanical strength increased.

5) Nanoparticles pile-up effect:

The use of nanomaterials in concrete could have adverse consequences, too. This may be due to poor distribution of nanoparticles in the mixture, a mass of nanoparticles in coming, and they form the cavities in the cement paste, thereby reducing the resistance (Especially in the case of MgO nano). This project deals with pile-up effect phenomena in mixed mortar and concrete, by using ultrasonic waves. SEM images taken from different levels of broken concrete confirm that nanomaterials had proper and homogeneous distribution in mortar and concrete mixes.

6) The use of Nanomaterials as injection grouts could allow significantly reducing the open porosity as well as the absorption of capillary water of existing walls while maintaining their integrity and structural quality, in order to achieve the goals of reducing primary energy consumption in the building envelope.

7) Significant energy savings can be achieved by the application of aerogel-enhanced systems, however generally at a high primary cost due to the not competitive price of aerogel.

In this research, the physical properties of more than 1400 concrete mixtures were investigated. The main goal was to find the optimal amount of Zinc Oxide (ZnO), Magnesium Oxide (MgO), and composite nanoparticle additives which can be added to the concrete mixtures. The compressive strength of concrete mixture and tensile strength can be increased by 25%. Further, the water permeability of the mixture was reduced by 40%. By reducing the water permeability, the thermal conductivity of the samples will be reduced. Thus, the energy consumption of the building can be drastically reduced.

Conflicts of Interest

The authors declare no conflicts of interest regarding the publication of this paper.

References

[1] Esmaeili, J. and Andalibi, K. (2013) Investigation of the Effects of Nano-Silica on the Properties of Concrete in Comparison with Micro-Silica. *International Journal of Nano Dimension*, **3**, 321-328.

[2] Lin, D.-F. and Tsai, M.-C. (2006) The Effects of Nanomaterials on Microstructures of Sludge Ash Cement Paste. *Journal of the Air & Waste Management Association*, **56**, 1146-1154. https://doi.org/10.1080/10473289.2006.10464537

[3] Behfarnia, K., Azarkeivan, A. and Keivan, A. (2013) The Effects of TiO_2 and ZnO Nanoparticles on Physical and Mechanical Properties of Normal Concrete. *Asian Journal of Civil Engineering*, **14**, 517-531.

[4] Jo, B.W., Kim, C.H., Tae, G.H. and Park, J.B. (2007) Characteristics of Cement Mortar with Nano-SiO_2 Particles. *Construction and Building Materials*, **21**, 1351-1355.

https://doi.org/10.1016/j.conbuildmat.2005.12.020

[5] Nazari, A. and Riahi, S. (2011) The Effects of TiO_2 Nanoparticles on Physical, Thermal and Mechanical Properties of Concrete Using Ground Granulated Blast Furnace Slag as Binder. *Materials Science and Engineering*: *A*, **528**, 2085-2092. https://doi.org/10.1016/j.msea.2010.11.070

[6] Senff, L., Tobaldi, D.M., Lucas, S., Hotza, D., Ferreira, V.M. and Labrincha, J.A. (2013) Formulation of Mortars with Nano-SiO_2 and Nano-TiO_2 for Degradation of Pollutants in Buildings. *Composites Part B*: *Engineering*, **44**, 40-47. https://doi.org/10.1016/j.compositesb.2012.07.022

[7] León, N., Massana, J., Alonso, F., Moragues, A. and Sánchez-Espinosa, E. (2014) Effect of Nano-Si_2O and Nano-Al_2O_3 on Cement Mortars for Use in Agriculture and Livestock Production. *Biosystems Engineering*, **123**, 1-11. https://doi.org/10.1016/j.biosystemseng.2014.04.009

[8] Sobolev, K. and Gutiérrez, M.F. (2005) How Nanotechnology Can Change the Concrete World. *American Ceramic Society Bulletin*, **84**, 14-17.

[9] Flores-Velez, L.M. and Dominguez, O. (2002) Characterization and Properties of Portland Cement Composites Incorporating Zinc-Iron Oxide Nanoparticles. *Journal of Materials Science*, **37**, 983-988. https://doi.org/10.1023/A:1014304131987

[10] Li, H., Xiao, H.-G. and Ou, J.-P. (2004) A Study on Mechanical and Pressure-Sensitive Properties of Cement Mortar with Nanophase Materials. *Cement and Concrete Research*, **34**, 435-438. https://doi.org/10.1016/j.cemconres.2003.08.025

[11] Li, H., Zhang, M.-H. and Ou, J.-P. (2006) Abrasion Resistance of Concrete Containing Nano-Particles for Pavement. *Wear*, **260**, 1262-1266. https://doi.org/10.1016/j.wear.2005.08.006

[12] Jalal, M., Pouladkhan, A., Harandi, O.F. and Jafari, D. (2015) Comparative Study on Effects of Class F Fly Ash, Nano Silica and Silica Fume on Properties of High Performance Self-Compacting Concrete. *Construction and Building Materials*, **94**, 90-104. https://doi.org/10.1016/j.conbuildmat.2015.07.001

[13] Navarro, V., *et al*. (2006) Characterization of the Water Flow through Concrete Based on Parameter Estimation from Infiltration Tests. *Cement and Concrete Research*, **36**, 1575-1582. https://doi.org/10.1016/j.cemconres.2005.11.015

[14] Chia, K.S. and Zhang, M.-H. (2002) Water Permeability and Chloride Penetrability of High-Strength Lightweight Aggregate Concrete. *Cement and Concrete Research*, **32**, 639-645. https://doi.org/10.1016/S0008-8846(01)00738-4

[15] Li, Z.W., Gao, W. and Reeves, R.J. (2005) Zinc Oxide Films by Thermal Oxidation of Zinc Thin Films. *Surface and Coatings Technology*, **198**, 319-323. https://doi.org/10.1016/j.surfcoat.2004.10.111

[16] Nivethitha, D. and Dharmar, S. (2016) Influence of Zinc Oxide Nanoparticle on Strength and Durability of Cement Mortar. *International Journal of Earth Sciences and Engineering*, **9**, 175-181.

[17] Xu, G., Shen, W., Huo, X., Yang, Z., Wang, J., Zhang, W. and Ji, X. (2018) Investigation on the Properties of Porous Concrete as Road Base Material. *Construction and Building Materials*, **158**, 141-148. https://doi.org/10.1016/j.conbuildmat.2017.09.151

[18] Sagadevan, S. and Koteeswari, P. (2015) Analysis of Structure, Surface Morphology, Optical and Electrical Properties of Copper Nanoparticles. *Journal of Nanomedicine Research*, **2**, 133-136. https://doi.org/10.15406/jnmr.2015.02.00040

[19] ASTM International (2012) ASTM C494. Standard Specification for Chemical Ad-

mixtures for Concrete. In: *Annual Book of ASTM Standards*, ASTM International, Conshohocken.

[20] ASTM International (2002) ASTM C-496. Standard Test Method for Splitting Tensile Strength of Cylindrical Concrete Specimens. In: *Annual Book of ASTM Standards*, Vol. 04.02, ASTM International, Conshohocken, 281-284.

[21] (1991) Recommended Practice for Proportioning Normal and Heavy-weight Concrete Mixtures. ACI 211.1, American Concrete Institute, Detroit.

[22] Baykasoğlu, A., Öztaş, A. and Özbay, E. (2009) Prediction and Multi-Objective Optimization of High-Strength Concrete Parameters via Soft Computing Approaches. *Expert Systems with Applications*, **36**, 6145-6155. https://doi.org/10.1016/j.eswa.2008.07.017

[23] Berardi, U. (2018) Aerogel-Enhanced Systems for Building Energy Retrofits: Insights from a Case Study. *Energy and Buildings*, **159**, 370-381. https://doi.org/10.1016/j.enbuild.2017.10.092

[24] Casini, M. (2016) Nano Insulating Materials and Energy Retrofit of Buildings. *AIP Conference Proceedings*, **1749**, Article ID: 020005. https://doi.org/10.1063/1.4954488